Effects of Cross-Linking on the Morphology of Structured Latex Particles. 1. Theoretical Considerations

Yvon G. Durant and Donald C. Sundberg*

Polymer Research Group, Department of Chemical Engineering, University of New Hampshire, Durham, New Hampshire 03824

Received February 8, 1996[⊗]

ABSTRACT: Cross-linking of the seed latex polymer introduces elastic forces into the thermodynamic analysis of the morphology of composite particles. By determining the elastic storage energy necessary to maintain a deformation within the seed latex particle (as in an occlusion of second-stage polymer), it can be combined with the interfacial energies internal to the particle and at its aqueous phase boundary to compute the total free energy of a specific particle morphology. At low levels of cross-linking it is found that the elastic and interfacial energies are of the same order of magnitude, with the final morphology determined by the balance between them. Elastic energies are dependent upon the state of deformation within the particle, and this makes the thermodynamic equilibrium morphology analysis dependent upon cross-link level, seed latex particle size, stage ratio (second polymer/seed polymer), and the interfacial tensions at the polymer/polymer and polymer/water interfaces. Computational results are presented which show the effects of each of these variables on the predicted morphology.

Introduction

The growing interest in latex particle morphology has recently resulted in a number of reports on the effect of different variables on the particle structure.[1−30] Among the variables reported are the polymer and monomer types, surfactants, initiator end groups, and process characteristics (batch and semibatch operations). Distinctly absent from the above list of variables is that of cross-linking of either or both of the polymers. Our purpose in this paper is to consider the effects of a cross-linked seed latex on the morphology of a composite particle in which the second-stage polymer is linear and is produced in a batch reaction environment.

We consider a seed latex particle which is *uniformly* cross-linked to a certain extent and swollen with second-stage monomer to a chosen level, short of saturation. Particularly interesting is the case in which the thermodynamics would favor an inverted core−shell particle (i.e. second-stage polymer as the core) when the seed latex was not cross-linked and to assess the effect of increasing cross-link levels of the seed polymer. Clearly, if the seed polymer is highly cross-linked, it will remain as a spherical core, with the second-stage polymer being forced to engulf it to some extent. The more interesting situation is to consider a lightly cross-linked seed polymer and to analyze the free energies separately associated with the elastic and interfacial forces which combine to determine the ultimate particle morphology. In particular, we would like to know the sensitivity of the morphology to the cross-link level and to be able to determine the minimum cross-link level to assure a core−shell structure, with the shell being the second-stage polymer.

When we consider a cross-linked seed latex particle which has been deformed due to the presence of a second phase, there will be elastic forces which result in a given amount of free energy, G_e, stored in the particle. This energy combines with that of the interfacial free energy to yield the total free energy of the particle, G. This can be expressed as

$$G = G_s + G_e + G° \tag{1}$$

where G is the total free energy of the particle, G_s is the interfacial energy, and $G°$ is the reference state energy. Equation 1 differs from that applied to our previous free energy analyses of latex particle morphology[11−14,17,18,29,30] only by the term G_e, and here we follow our previous approach in which we consider the differences between G for a variety of particle structures. In this paper, we will restrict our considerations to core−shell (CS), inverted core−shell (ICS), and occluded (OCC) structures.

Theoretical Considerations of the Elastic Energy

The elastic forces are dependent on four dominant parameters: T, the temperature; M_c/M, the molecular weight between cross-links; α, the displacement gradient tensor (the state of deformation of the network can be expressed as $a_{ij} = dx_i/dx_j$, where x_i and x_j are the coordinates of a point in the deformed and undeformed states, respectively); and b, the stiffness of the chain.

This elastic term, G_e, is considered to be a function of M_c, α, b, and T. According to the fundamental thermodynamic definitions,

$$\text{stored energy} = E = \int f\,dx = U$$

and at constant temperature and pressure $G_e = U$. Here U is the internal energy.

The stored internal energy can be analyzed by using the framework provided by solid mechanics as it is applied to the elastic energy of a Hookean solid under an external stress. Such a solid (in this case our cross-linked seed polymer) can be deformed (externally) in three dimensions X, Y, and Z. The force resulting from the external stress can be written as a vector in space.

$$\vec{F} = \vec{F}_X + \vec{F}_Y + \vec{F}_Z = \vec{\imath}F_X + \vec{j}F_Y + \vec{k}F_Z \tag{2}$$

Vectors $\vec{\imath}$, $\vec{j}$, and $\vec{k}$ represent the unit vectors in each dimension X, Y, and Z. The corresponding stored energy for a deformation from (x_0,y_0,z_0) to (x_1,y_1,z_1) is

[⊗] Abstract published in *Advance ACS Abstracts,* October 1, 1996.

S0024-9297(96)00200-8 CCC: $12.00

$$E = \int_{x_0}^{x_1} F_x \, dx + \int_{y_0}^{y_1} F_y \, dy + \int_{z_0}^{z_1} F_z \, dz \qquad (3)$$

According to statistical analysis of isolated chains,[31] the force in each dimension can be expressed as

$$F_x \cong \frac{kT}{l}\left[3\frac{x}{nl} + \frac{9}{5}\left(\frac{x}{nl}\right)^3 + \frac{297}{175}\left(\frac{x}{nl}\right)^5\right] \qquad (4)$$

where k = Boltzmann's constant, l is the bond length, and n is the number of repeat units between cross-links, with similar expressions for F_y and F_z. Under isotropic assumptions, we have the two relations

$$bnl^2 = R_0^{\,2} = x_0^{\,2} + y_0^{\,2} + z_0^{\,2} \qquad (5)$$

$$x_0^{\,2} = y_0^{\,2} = z_0^{\,2} \qquad (6)$$

where $1 \le b \le 10$ (ref 32) and $n = M_c/M$, with M the molecular weight of the repeating unit. The coefficient b represents the stiffness of the bond between the atomic constituents of the polymeric chain. A value of 1 corresponds to a freely rotating chain, while increasing values represent higher and higher restrictions to bond rotation. A more detailed analysis of the bond stiffness is given in the Appendix.

If a cubic unit volume originally had dimensions x_0,y_0,z_0 and a force F_x is applied, under the assumptions of incompressibility and isotropic conditions, we obtain new dimensions for the unit volume, $\alpha x_0, y_0/\alpha^{1/2}, z_0/\alpha^{1/2}$, where α represents the deformation. The energy stored in this unit of volume is then

$$E = \int_{x_0}^{\alpha x_0} F_x \, dx + \int_{y_0}^{y_0/a^{1/2}} F_y \, dy + \int_{z_0}^{z_0/\alpha^{1/2}} F_z \, dz \qquad (7)$$

After combination and rearrangement of eqs 4−7, one obtains

$$E = \frac{\rho RT}{M_c}\left(1 - 2\frac{M_c}{M_w}\right)\left[(\alpha^2 + 2\alpha^{-1} - 3)\left(\frac{b}{2}\right) + (\alpha^4 + 2\alpha^{-2} - 3)\left(\frac{1}{20}\right)\left(\frac{M}{M_c}\right)b^2 + (\alpha^6 + 2\alpha^{-3} - 3)\left(\frac{11}{1050}\right)\left(\frac{M}{M_c}\right)^2 b^3\right] \qquad (8)$$

where ρ is the density of the polymer, R is the gas constant, T is the temperature, M_c is the molecular weight between cross-links, M_w is the molecular weight of the un-cross-linked chain, and M is the molecular weight of the monomer.

Application to the Case of One Occlusion in a Cross-Linked Sphere, or Inverted Core−Shell (ICS)

Figure 1 shows a geometric representation of the initial sphere and a postformed inverted core−shell particle. r_s is the radius of the original sphere (cross-linked seed), and r_0 is the radius of the occlusion. The radial distance r is then transposed in the expanded sphere to a new radius r'. For a layer of thickness dr at radius r, we have the following energy based on an integration of eq 8:

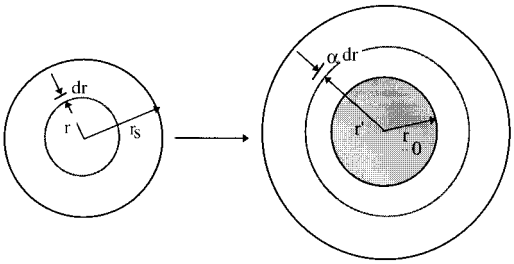

Figure 1. Geometrical representation of the expansion of the seed particle of radius r_s to an inverted core−shell (ICS) with a core radius r_0. r' represents the displacement of an arbitrary point in the seed particle represented by r. dr and α dr are the corresponding layer thicknesses.

$$G_e = \int_0^{r_s} E(4\pi r^2)\, dr = 4\pi\frac{\rho RT}{M_c}\left(1 - 2\frac{M_c}{M_w}\right)\int_0^{r_s}\left[(\alpha^2 + 2\alpha^{-1} - 3)\left(\frac{b}{2}\right) + (\alpha^4 + 2\alpha^{-2} - 3)\left(\frac{1}{20}\right)\left(\frac{M}{M_c}\right)b^2 + (\alpha^6 + 2\alpha^{-3} - 3)\left(\frac{11}{1050}\right)\left(\frac{M}{M_c}\right)^2 b^3\right] r^2\, dr \qquad (9)$$

The deformation of a layer at radius r with a thickness dr is such that the new layer is at radius r' and of thickness dr'. With the conservation of the volume (i.e. at constant density), we obtain

$$4\pi r^2\, dr = 4\pi r'^{\,2}\, dr' \qquad (10)$$

Because the sphere of the inner core is of radius r_0, we have the volumetric relation

$$\frac{4}{3}\pi r^3 + \frac{4}{3}\pi r_0^{\,3} = \frac{4}{3}\pi r'^{\,3} \qquad (11)$$

The radial deformation is by definition and analogy to αx_0, d$r' = \alpha$ dr. Thus we finally obtain from eqs 10 and 11

$$\alpha = \left(1 + \left(\frac{r_0}{r}\right)^3\right)^{-2/3} \qquad (12)$$

It is now possible to calculate the stored energy, G_e, from eqs 3 and 6.

Numerical Application

Due to the nature of eqs 9 and 12, only numerical solutions are possible. Furthermore, the elastic energy is dependent upon the size of the seed particle, r_s, and the amount of second-stage polymer (represented by r_0). We have solved eqs 9 and 12 by creating two master curves for G_e which depend on r_s, r_0, and the parameter K. K combines all of the constants within eq 9 which do not include radius and reflects the level of cross-linking in the seed polymer.

$$K = 4\pi\frac{\rho RT}{2M_c}\left(1 - 2\frac{M_c}{M_w}\right) \qquad (13)$$

Equation 9 can be separated into two parts, A and B, as follows:

$$A = \int_0^{r_s}[\alpha^2 + 2\alpha^{-1} - 3]r^2\, dr \qquad (14)$$

$$B = 2\int_0^{r_s}(\alpha^4 + 2\alpha^{-2} - 3)\frac{1}{20}r^2\,dr \qquad (15)$$

$$C = 2\int_0^{r_s}(\alpha^6 + 2\alpha^{-3} - 3)\frac{11}{1050}r^2\,dr \qquad (16)$$

As such, G_e can now be expressed as

$$G_e = K\left[Ab + B\frac{M}{M_c}b^2 + C\left(\frac{M}{M_c}\right)^2 b^3\right] \qquad (17)$$

We further note that B and C can be much larger than A at high extensions (i.e. a large value of r_0).

Equation 14 was solved for A as a function of (r_0/r_s) noting that α and (r_0/r_s) are related as in eq 12. This solution is represented graphically in Figure 2 as the (●) points for the axes $\log(A/r_s^3)$ and $\log(r_0/r_s)$. For future computational convenience, we have placed a third-order polynomial through these points, and the resulting equation is shown within Figure 2.

Figure 3 represents the results of a similar treatment of B and C from eqs 15 and 16. We use the polynomials later in this paper to compute G_e for use in eq 1.

Extension of the ICS Case to Multiple Occusions

It is possible to extend the model of the elastic energy of the previous inverted core−shell (ICS) to that of an occluded structure with n occlusions (OCC_n). It has been assumed in this model, as a working hypothesis, that the elastic energy for a two-phase particle with n occlusions (OCC_n) can be mathematically represented as the sum of the elastic energies for n individual inverted core−shell particles symbolically shown in Figure 4. The radius of the equivalent core of each single ICS is then defined by the relation $r_0' = r_0/n^{1/3}$.

If we name the elastic energy G_e of eq 9 G_e^1 because it is the energy of a particle with one occlusion, we can write the energy of a structure with n occlusions as G_e^n. While utilizing eq 9 to determine G_e^n, it needs to be remembered that the "core" of each of the ICS particles in Figure 4 has the radius r_0 as noted above. Thus G_e^n can be written as

$$G_e^{\,n} = nG_e^{\,1} \qquad (18)$$

with the n individual r_0's given by $r_0/n^{1/3}$. This procedure allows one to use the polynomials described in the previous section with r_0 replaced by $r_0/n^{1/3}$.

Change in Free Energy

Our previous publications have used a reference free energy state as that of the initial seed particle. We found that for the cross-linking application it was more practical to use the free energy of the core−shell (CS) structure as reference. In other words, we calculate the free energy of transforming a CS into another structure as shown in Figure 5. In order to predict the most stable morphology, the difference of free energy between a CS and a particle with n occlusions (OCC_n) is calculated. Recall that OCC_1 is an ICS structure. The standard free energy $G°$ is the same in both the initial and final states. The minimum of free energy as a function of n will give the prediction for the most stable morphology (most stable OCC_n). Because of our new reference state, if this relative free energy is positive, the most stable structure is a CS particle. If it is negative, an ICS is most stable.

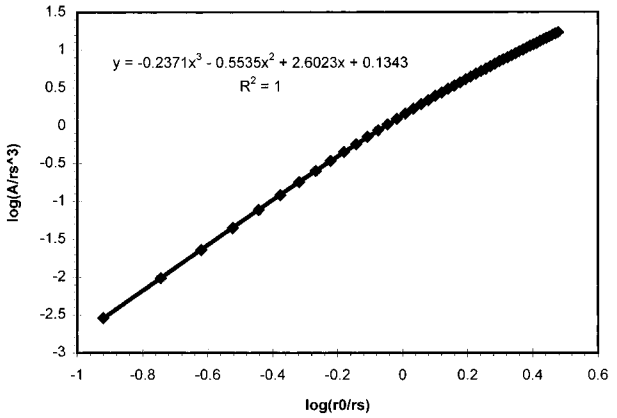

Figure 2. Master curve A on a log−log plot fitted with a third-degree polynomial.

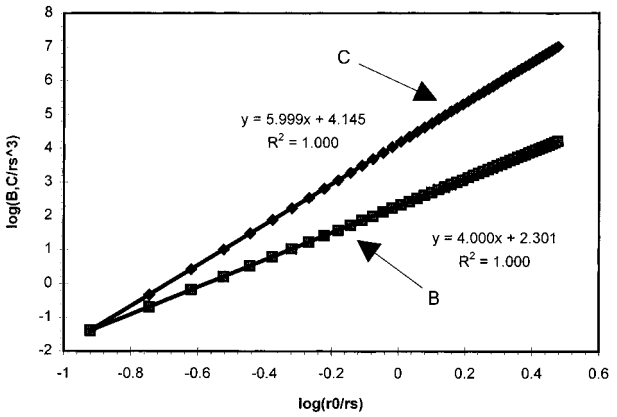

Figure 3. Master curves B and C on a log−log plot fitted by linear regression.

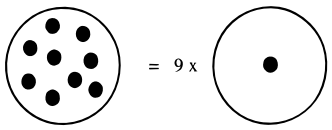

Figure 4. Particle with 9 occlusions represented (for its elasticity) as the sum of 9 simpler structures.

The surface energy equations of the two morphological structures of Figure 5 and their difference, ΔG_s, are shown below.

$$\Delta G_{OCC_n} = \gamma_{P_1/W}[4\pi(r_0^{\,3} + r_s^{\,3})^{2/3}] + n\gamma_{P_1/P_2}\left[4\pi\left(\frac{r_0}{n^{1/3}}\right)^2\right] \qquad (19)$$

$$\Delta G_{CS} = \gamma_{P_2/W}[4\pi(r_0^{\,3} + r_s^{\,3})^{2/3}] + \gamma_{P_1/P_2}(4\pi r_s^{\,2}) \qquad (20)$$

$$\Delta G_s = \Delta G_{OCC_n} - \Delta G_{CS} \qquad (21)$$

$$\Delta G_s = 4\pi[(r_s^{\,3} + r_0^{\,3})^{2/3}(\gamma_{P_1/W} - \gamma_{P_2/W}) + \gamma_{P_1/P_2}(n^{1/3}r_0^{\,2} - r_s^{\,2})] \qquad (22)$$

Here, $\gamma_{P_1/W}$ is the interfacial tension at the polymer 1 (seed polymer)/water interface, $\gamma_{P_2/W}$ that at the polymer 2/water interface, and γ_{P_1/P_2} that between the two polymers. These can be used in conjunction with eq 18 for G_e^n to describe the free energy change of the process shown in Figure 5. Note that the reference CS particle has no elastic energy, as only the seed polymer is cross-linked. Thus

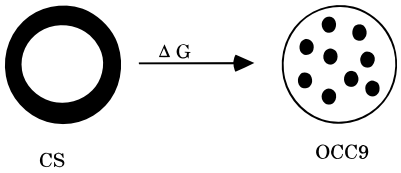

Figure 5. Free energy pathway for transforming a core−shell particle into an occluded structure (OCC).

$$\Delta G = \Delta G_e + G_s \tag{23}$$

$$\Delta G_e = G_e^{OCC_n} - G_e^{CS} + nG_e^{n} - 0 \tag{24}$$

$$\Delta G = nG_e^{n} + 4\pi[(r_s^3 + r_0^3)^{2/3}(\gamma_{P_1/W} - \gamma_{P_2/W}) + \gamma_{P_1/P_2}(n^{1/3}r_0^2 - r_s^2)] \tag{25}$$

Given values of the various interfacial tensions, the seed latex particle size (r_s), and the amount of second-stage polymer (equivalently r_0), one can use eq 25 to determine whether the single or multiple occlusion structure is thermodynamically favored over a core−shell arrangement. Since the CS was taken as the reference state, positive values of ΔG in eq 24 predict that the CS is preferred, while negative values predict that an ICS or occluded structure is preferred.

Discussion

In contrast to the free energy predictions for composite latex particles comprised of linear polymers, those for cross-link seed latices are not independent of particle size. The elastic energy term makes the seed particle size and amount of second-stage polymer important factors and creates some difficulties in presenting results in a simple fashion. This has caused us to develop graphical output which we describe as domain maps to identify preferred morphologies. Several of them are described below and unless stated to the contrary utilize the following set of interfacial tensions:

$$\gamma_{P_1/W} = 10.7 \text{ mN/m}; \quad \gamma_{P_2/W} = 13.2 \text{ mN/m}; \quad \gamma_{P_1/P_2} = 1.7 \text{ mN/m}$$

These values reasonably represent the PMMA (P_1)/PS (P_2) system at full conversion and at 60 °C with sodium dodecyl sulfate (SDS) as surfactant. We chose the values because without cross-linking, the preferred morphology is ICS, and with increasing levels of cross-linking, we can contrast the elastic and interfacial energy terms and distinguish their effects on particle structure. The first application presents the effect of stage ratio (volume of P_2:volume of P_1) on the total free energy of the particle at the different cross-link densities. Figure 6 shows the results of several sets of computations for which the stage ratio is changed for several cross-link levels. The seed particle diameter in these calculations is 200 nm. When the curve is below zero energy, the predicted morphology is ICS (single core for this figure) and when it is above zero, a core−shell is predicted. Thus for a cross-link density representative of $M_c/M = 1000$, the morphology is predicted to remain as an ICS until the stage ratio exceeds 180%, whereupon further increases of second-stage polymer causes a switch to core−shell morphology. Similar results for other cross-link densities are also shown in Figure 6.

It is helpful to view the zero energy level as the border between ICS and CS morphologies for the seed particle

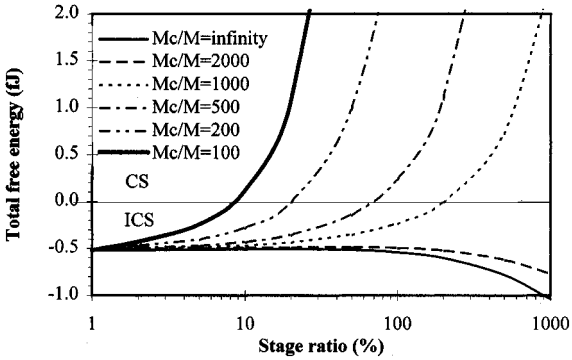

Figure 6. Effect of the stage ratio on the total free energy at different levels of cross-linking density. The seed particle diameter is 200 nm, and the interfacial tensions are $\gamma_{P_1/W} = 10.7$ mN/m, $\gamma_{P_2/W} = 13.2$ mN/m, and $\gamma_{P_1/P_2} = 1.7$ mN/m. fJ = 10^{-15} J.

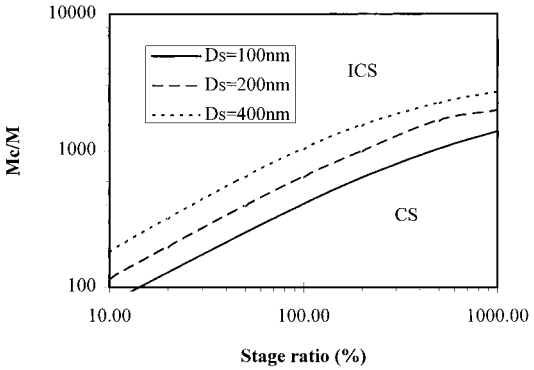

Figure 7. Morphology domain map. The lines represent the separation between ICS (top left) and CS (bottom right) for different seed particle sizes. These lines have been calculated with the following interfacial tensions: $\gamma_{P_1/W} = 10.7$ mN/m, $\gamma_{P_2/W} = 13.2$ mN/m, and $\gamma_{P_1/P_2} = 1.7$ mN/m.

size considered. When this is done for different seed latex particle sizes, a more easily interpreted plot can be obtained as in Figure 7. Here each line represents the border between ICS and CS for a given seed particle size. As an example of its utility, consider a seed with $D_s = 200$ nm cross-linked to $M_c/M = 1000$ and with a stage ratio of 100%. Under these conditions, we predict an ICS structure. Increasing cross-linking such that $M_c/M = 500$ or increasing the stage ratio to just above 200% causes a shift to CS structure. Figure 7 clearly shows that the larger the seed latex particle, the more easily elastic forces cause CS structures to gain favor.

Given that the results presented in Figures 6 and 7 are only valid for the particular set of interfacial tensions noted above, it is of interest to see how these interfacial tensions affect the morphology in cross-linked systems. Again, because of the new dependence of the free energies on seed latex particle size and stage ratio that the cross-linking brings about, the presentation of results is somewhat difficult (i.e. there are too many variables to display them in a single figure). In Figure 8 we have plotted the polymer/polymer interfacial tension, γ_{P_1/P_2}, against the *difference* between the polymer/water interfacial tensions, i.e. $\gamma_{P_2/W} - \gamma_{P_1/W}$, at different levels of cross-linking, seed particle diameter, and stage ratio. The lines in the figure represent the border between ICS (single core) and CS for the particular cross-linking level. As seen here, for a fixed value of γ_{P_1/P_2}, increasing $\gamma_{P_2/W}$ as compared to $\gamma_{P_1/W}$ causes the morphology to shift from ICS arrangements toward CS. This is not unexpected, as the same type of behavior is found in non-cross-linked systems. Alternatively, for a

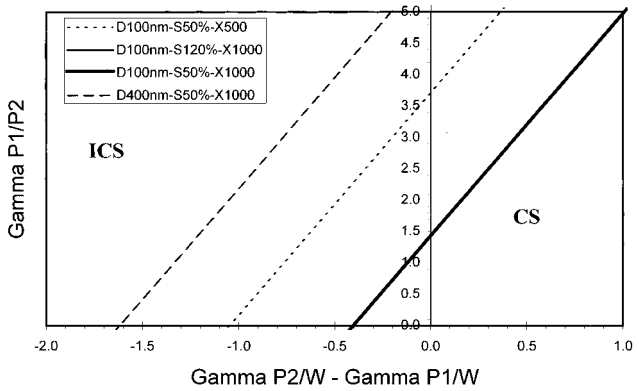

Figure 8. Morphology domain map of the effect of the interfacial tensions. By selecting a set of interfacial tensions ($\gamma_{P_2/W} - \gamma_{P_1/W}$) and γ_{P_1/P_2} and selecting the line relevant to the seed particle diameter (D), the stage ratio (S), and the cross-linking density ($X = M_c/M$), one can determine the most stable morphology of such a system.

fixed ($\gamma_{P_2/W} - \gamma_{P_1/W}$) value, increasing γ_{P_1/P_2} causes the morphology to shift from CS toward ICS. The nature of eq 25 implies that straight lines separate the ICS and CS domains in Figure 8. A change in cross-linking density affects only the elastic energy term and consequently yields a line parallel to the base case (thick continuous line). On the contrary, a change in stage ratio will modify both the elastic energy and the surface energy, yielding a straight line of different slope and intercept as compared to the base case. The adjustment of any parameter increasing the relative dimension of the elastic energy compared to the surface energy will increase the morphology domain attributed to CS.

Occluded Systems

Winzor[17,18] considered occluded particles when making equilibrium morphology predictions for non-cross-linked latices and showed, as expected, that a single occlusion was always more thermodynamically favorable than multiple occlusions. However, there was not a large difference in the total energies of occluded and nonoccluded systems, and those energies are asymptotically bound as the number of occlusions is increased. Given this situation, it is useful to investigate the influence of seed latex cross-linking on the likelihood of predicting occluded structures with lower free energy than fully phase-separated particles.

Considering an ICS structure, as the number of equal-sized occlusions increases (at fixed stage ratio), the interfacial free energy also increases due to the greater internal interfacial area. On the other hand, the elastic energy decreases (see eq 18) due to the necessarily smaller size of the occlusions. Both of these energies are asymptotically limited and under the right circumstances can conceivably add together in such a way as to describe a total free energy which passes through a minimum as the number of occlusions increases.

Figures 9−11 show the elastic, interfacial, and total free energies as a function of the number of occlusions ($n = 1$ being an ICS) for different levels of cross-linking. In all these figures, DGel, DGs, and DGtot stand for ΔG_{el}, ΔG_s, and ΔG, respectively, and the energy scale is in femtojoules (fJ $= 10^{-15}$ J). All figures are based on a seed particle diameter of 200 nm, a swelling ratio of 50%, and the interfacial tensions noted at the beginning of this discussion. At a low cross-linking level of $M_c/M = 2000$, Figure 9 shows that the interfacial free energy increases much more rapidly than the elastic free

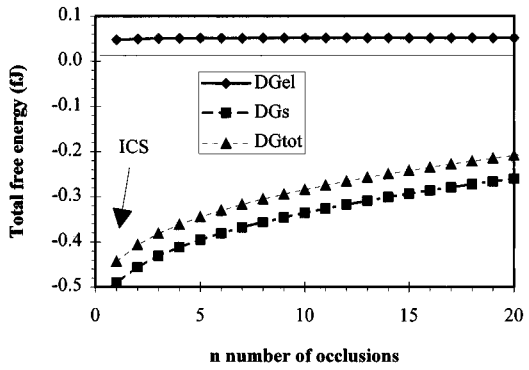

Figure 9. Free energy as a function of the number of occlusions in a two-phase cross-linked particle. Swelling ratio = 50%, seed particle diameter = 200 nm, $M_c/M = 2000$, $\gamma_{P_1/W}$ = 10.7 mN/m, $\gamma_{P_2/W}$ = 13.2 mN/m, and γ_{P_1/P_2} = 1.7 mN/m.

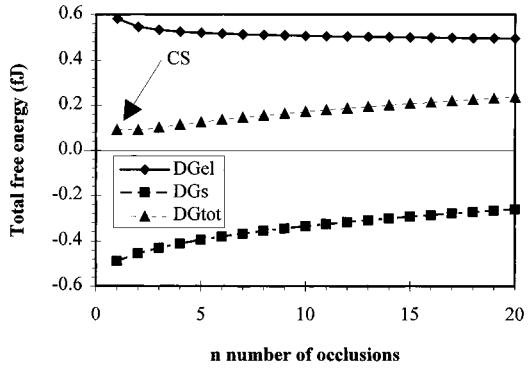

Figure 10. Free energy as a function of the number of occlusions in a two-phase cross-linked particle. Swelling ratio = 50%, seed particle diameter = 200 nm, $M_c/M = 350$, $\gamma_{P_1/W}$ = 10.7 mN/m, $\gamma_{P_2/W}$ = 13.2 mN/m, and γ_{P_1/P_2} = 1.7 mN/m.

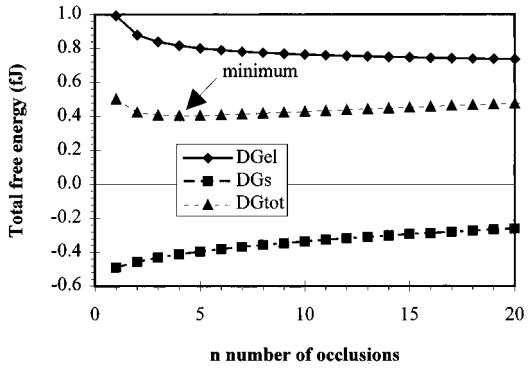

Figure 11. Free energy as a function of the number of occlusions in a two-phase cross-linked particle. Swelling ratio = 50%, seed particle diameter = 200 nm, $M_c/M = 250$, $\gamma_{P_1/W}$ = 10.7 mN/m, $\gamma_{P_2/W}$ = 13.2 mN/m, and γ_{P_1/P_2} = 1.7 mN/m.

energy decreases with larger numbers of occlusions, resulting in the prediction of a single occlusion (ICS) being thermodynamically favored. The situation changes dramatically when the cross-link level is increased to a value of $M_c/M = 350$, as in Figure 10. Here the total free energies are always above zero and monotonically increasing, indicating a strong preference for CS structure. Further change in the cross-linking to M_c/M = 250 (Figure 11) produces an interesting situation in which the total free energy, while always positive and suggesting a CS arrangement, passes through a minimum at 4 occlusions. This energy minimum is not considered to be useful as the total free energy at the minimum is well above zero and CS structure is the strongly favored equilibrium state.

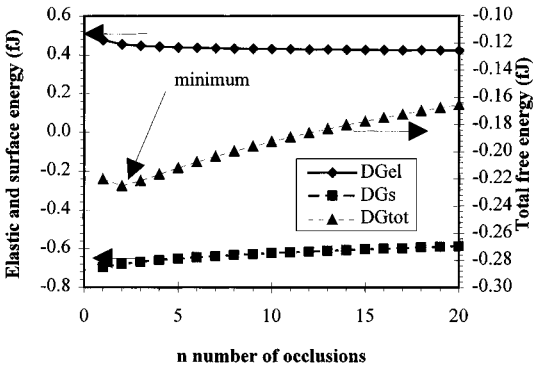

Figure 12. Free energy as a function of the number of occlusions in a two-phase cross-linked particle. Swelling ratio = 50%, seed particle diameter = 200 nm, $M_c/M = 400$, $\gamma_{P_1/W} =$ 10 mN/m, $\gamma_{P_2/W} = 14$ mN/m, and $\gamma_{P_1/P_2} = 0.8$ mN/m. A structure with 2 occlusions is the most stable morphology.

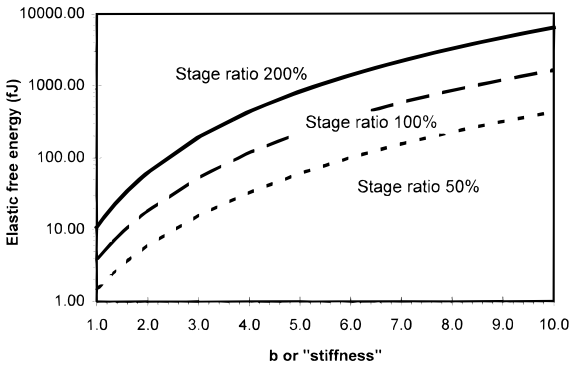

Figure 13. Effect of the polymer stiffness *b* on the elastic free energy for two different stage ratios for a seed particle of 200 nm and $M_c/M = 400$.

Because it was of interest for us to look further for situations in which occluded structures would be thermodynamically favored, we changed interfacial tensions, cross-link levels, seed diameter, and stage ratio over wide ranges. Figure 12 shows the results for a seed latex 200 nm in diameter with $M_c/M = 400$, a swelling ratio of 50%, and a particular set of interfacial tensions ($\gamma_{P_1/W} = 10$ mN/m; $\gamma_{P_2/W} = 14$ mN/m; $\gamma_{P_1/P_2} = 0.8$ mN/m). The total energies are always negative, but only by a small amount due to the very close (but of opposite sign) values of the interfacial and elastic free energies. Here there is a clearly discerned minimum energy at 2 occlusions. This condition is created because of the low value of γ_{P_1/P_2} and the significant level of cross-linking. At this point in time we cannot suggest that the particular values of interfacial tensions represent a practical situation and thus cannot conclude that cross-linking creates the real possibility of thermodynamically favored occluded structures. Clearly under dynamic, nonequilibrium conditions as found in rapid polymerization systems there will often be the production of occluded particles. The work presented above can be used to compute how far from equilibrium conditions any such structure exists and to give some idea of the propensity for such a particle to change its structure with time.

Conclusions

The effects of seed latex cross-linking on the resultant equilibrium morphology of composite particles can be computed from the basic mechanics of amorphous polymers as applied to rubberlike elasticity. At low levels of cross-linking, the elastic energy term in the free energy expression is of the same order of magnitude as the interfacial energy terms. Under these conditions, the control of particle morphology is achieved via a balance of these energies. The consideration of elastic forces results in free energy expressions which are dependent upon the seed latex particle size, cross-link level, interfacial tensions, and the stage ratio of polymers. In contrast, consideration of only interfacial forces (as in non-cross-linked systems) allows for morphology predictions which are independent of particle size. It appears from our calculations that very small levels of cross-linking will have a rather large effect upon latex particle morphology.

Acknowledgment. We are grateful for the financial support provided by the University of New Hampshire and the Centre National de la Recherche Scientifique (LCPP Lyon, France). We also wish to thank Professor Claire Durant for useful mathematical discussions.

Appendix

As noted earlier in this paper, the deformation force created by an occlusion of second-stage polymer is dependent upon the stiffness of the deformed polymer chains. In eq 5 this chain stiffness is characterized by the parameter *b*, and its value was taken to be 1.0 for all calculations presented earlier. This value represents a freely rotating chain, while most polymers have values reported in the 4−10 range.[32] In Figure 13 we have shown the effect of changing the value of *b* on the elastic free energy (via eq 8) for the conditions noted in the figure legend. Clearly, an increase in chain stiffness should increase the deformation free energy for a given condition, and Figure 13 demonstrates that quantitative relationship for two different stage ratios. Application with *b* greater than 1.0 will therefore increase the influence of cross-linking on equilibrium morphology and make core−shell structures more readily achievable despite potentially adverse interfacial tension conditions.

References and Notes

(1) Lee, D. I. *ACS Symposium Series 165*; American Chemical Society: Washington, DC, 1981; p 405.
(2) Lee, D. I.; Ishikawa, T. *J. Polym. Sci., Polym. Chem. Ed.* **1983**, *21*, 147.
(3) Muroi, S.; Hashimoto, H.; Hosoi, K. *J. Polym. Sci., Polym. Chem. Ed.* **1983**, *22*, 1365.
(4) Okubo, M.; Katsuta, Y.; Matsumoto, T. *J. Polym. Sci., Polym. Lett. Ed.* **1980**, *18*, 481.
(5) Okubo, M.; Ando, M.; Yamada, A.; Katsuta, Y.; Matsumoto, T. *J. Polym. Sci., Polym. Lett. Ed.* **1981**, *19*, 143.
(6) Okubo, M.; Katsuta, Y.; Matsumoto, T. *J. Polym. Sci., Polym. Lett. Ed.* **1982**, *20*, 45.
(7) Stutman, D. R.; Klein, A.; El-Aasser, M. S.; Vanderhoff, J. W. *I&EC Prod. Res. Dev.* **1985**, *24*, 404.
(8) Cho, I.; Lee, K.-W. *J. Appl. Polym. Sci.* **1985**, *30*, 1903.
(9) Lee, S.; Rudin, A. *Makromol. Chem., Rapid Commun.* **1989**, *10*, 655.
(10) Lee, S.; Rudin, A. *J. Polym. Sci., Part A: Polym. Chem.* **1992**, *30*, 2211.
(11) Berg, J.; Sundberg, D. C.; Kronberg, B. J. *Polym. Mater. Sci. Eng.* **1986**, *54*, 367.
(12) Berg, J.; Sundberg, D. C.; Kronberg, B. J. *Microencapsulation* **1989**, *6*, 327.
(13) Sundberg, D. C.; Cassasa, A. J.; Pantazopoulos, J.; Muscato, M. R.; Kronberg, B.; Berg, J. *J. Appl. Polym. Sci.* **1990**, *41*, 1425.
(14) Muscato, M. R.; Sundberg, D. C. *J. Polym. Sci., Polym. Phys. Ed.* **1991**, *29*, 102.
(15) Dimonie, V. L.; El-Aasser, M. S.; Vanderhoff, J. W. *IACES Polym. Mater. Sci. Eng.* **1988**, *58*, 821.
(16) Jonsson, J.-E. L.; Hassander, H.; Jansson, L. H.; Tšrnell, B. *Macromolecules* **1991**, *24*, 126.

(17) Winzor, C. L.; Sundberg, D. C. *Polymer* **1992**, *33*, 3797.
(18) Winzor, C. L.; Sundberg, D. C. *Polymer* **1992**, *33*, 4269.
(19) Chen, Y. C.; Dimonie, V. L.; El-Aasser, M. S. *Macromolecules* **1991**, *24*, 3779.
(20) Chen, Y. C.; Dimonie, V. L.; El-Aasser, M. S. *J. Appl. Polym. Sci.* **1992**, *45*, 487.
(21) Chen, Y. C.; Dimonie, V. L.; El-Aasser, M. S. *J. Appl. Polym. Sci.* **1992**, *46*, 691.
(22) Chen, Y. C.; Dimonie, V. L.; Shaffer, O. L.; El-Aasser, M. S. *Polym. Int.* **1992**, *30*, 185.
(23) Sundberg, E. J.; Sundberg, D. C. *J. Appl. Polym. Sci.* **1993**, *47*, 1277.
(24) Rosen, S. L. *J. Appl. Polym. Sci.* **1973**, *17*, 1805.
(25) Min, T. I.; Klein, A.; El-Aasser, M. S.; Vanderhoff, J. W. *J. Polym. Sci., Polym. Chem. Ed.* **1983**, *21*, 2845.
(26) Merkel, M. P.; Dimonie, V. L.; El-Aasser, M. S.; Vanderhoff, J. W. *J. Polym. Sci., Part A: Polym. Chem.* **1987**, *25*, 1755.
(27) Hourston, D. J.; Satgurunathan, R.; Varnma, H. *J. Appl. Polym. Sci.* **1986**, *31*, 1955.
(28) Hourston, D. J.; Satgurunathan, R.; Varnma, H. *J. Appl. Polym. Sci.* **1987**, *33*, 215.
(29) Durant, Y. G.; Sundberg, D. C. *J. Appl. Polym. Sci.* **1995**, *57*, 1607.
(30) Sundberg, D. C.; Durant, Y. G. *Macromol. Symp.* **1995**, *92*, 43.
(31) Schultz, J. M. *Polymer Materials Science*; Prentice-Hall: Englewood Cliffs, NJ, 1974; pp 306−316.
(32) Flory, P. J. *Statistical Mechanics of Chain Molecules*; John Wiley and Sons: New York, 1969; pp 35−42.

MA960200O